Cell Reports, Volume *37*

Supplemental information

Targeting glioblastoma signaling and metabolism with a re-purposed brain-penetrant drug

Junfeng Bi, Atif Khan, Jun Tang, Aaron M. Armando, Sihan Wu, Wei Zhang, Ryan C. Gimple, Alex Reed, Hui Jing, Tomoyuki Koga, Ivy Tsz-Lo Wong, Yuchao Gu, Shunichiro Miki, Huijun Yang, Briana Prager, Ellis J. Curtis, Derek A. Wainwright, Frank B. Furnari, Jeremy N. Rich, Timothy F. Cloughesy, Harley I. Kornblum, Oswald Quehenberger, Andrey Rzhetsky, Benjamin F. Cravatt, and Paul S. Mischel

Figure S1

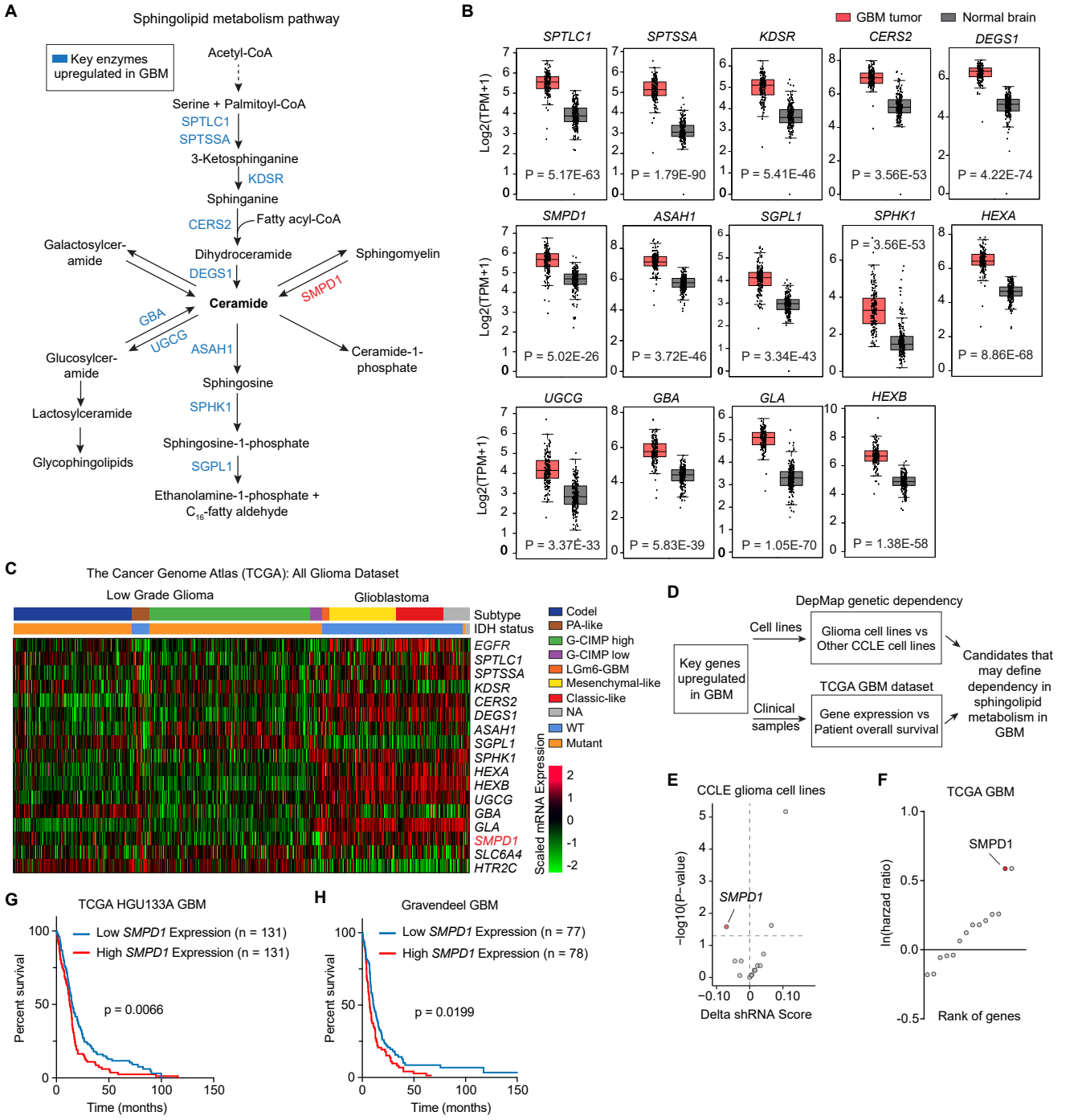

Figure S1. GBMs Are Highly Dependent on Sphingolipid Metabolism, Related to Figure 1

(A) Schematic pathways of sphingolipid metabolism.

(B) 14 coding genes of key enzymes in the sphingolipid metabolism pathway are highly expressed in GBM tumors (TCGA) in comparing with normal brains (GTEX).

(C) Heatmap of gene expression in the merged cohort of low-grade glioma and glioblastoma of TCGA datasets.

(D) Outline of the strategy utilized for identifying metabolic dependency of GBM in the sphingolipid pathway.

(E) Gene dependency analysis of 14 upregulated genes (B) in the sphingolipid metabolism pathway from the DepMap dataset. Glioma cells show a much more significant dependency on *SMPD1* than other sphingolipid metabolic genes.

(F) Rank of genes with the association (hazard ratio) between mRNA expression and overall survival of GBM patients from the TCGA dataset. High *SMPD1* expression is significantly correlated with poor overall survival of GBM patients.

(G and H) Kaplan-Meier analysis of overall survival in GBM patients with high (top 25%) or low (bottom 25%) *SMPD1* mRNA expression in the TCGA HGU133A GBM and Gravendeel GBM cohorts.

Two-tailed Student's t-test for (B) and (E). Log-rank test for (G) and (H). The median value (center line), the min and max (whiskers), and the 25th and 75th percentiles (box perimeters) are presented in (B).

Figure S2

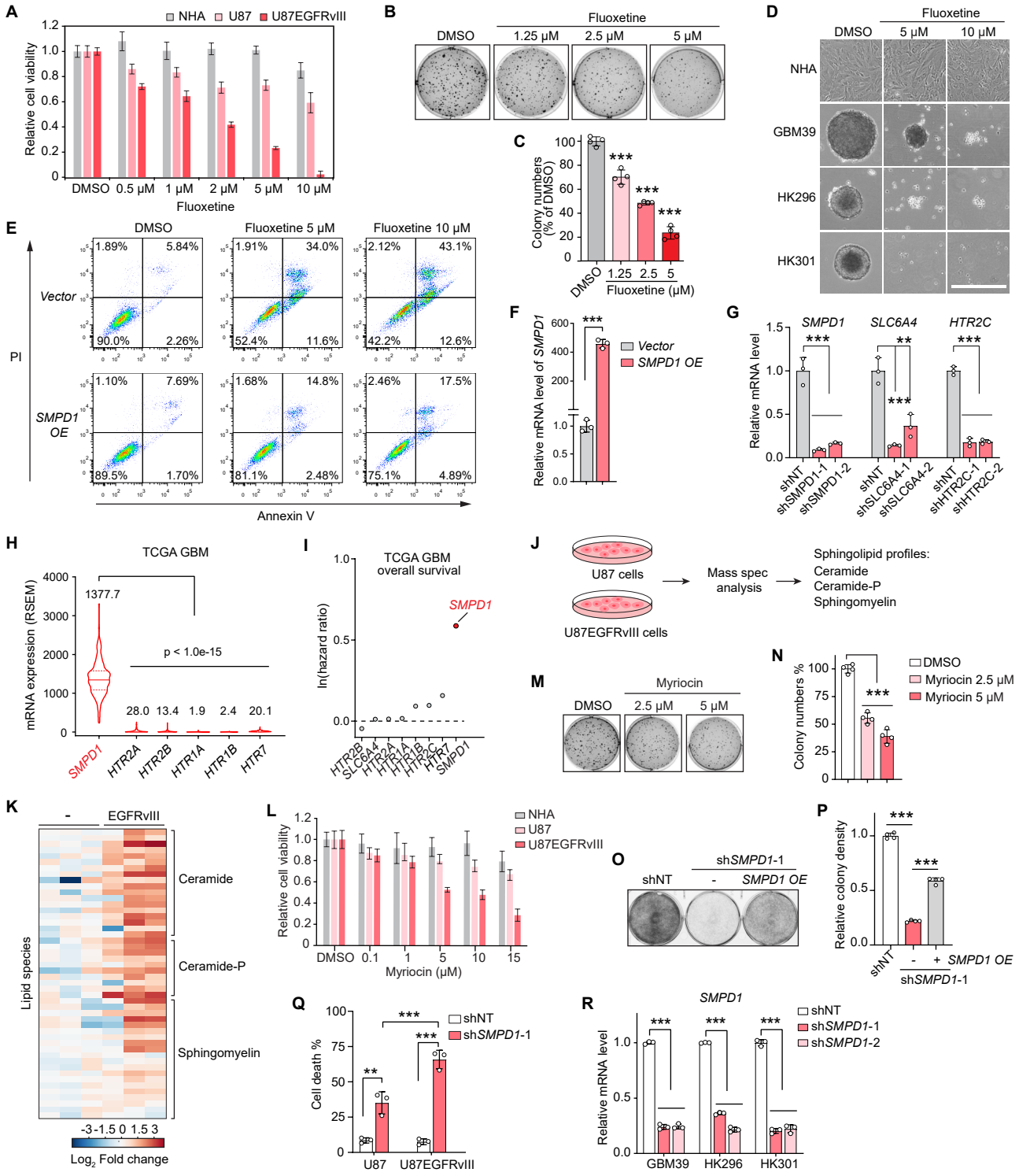

Figure S2. Fluoxetine Selectively Kills GBM Cells through SMPD1 Inhibition, Related to Figure 1 and 2

(A) Relative cell viability of normal human astrocytes (NHA), U87, and U87 cells expressing *EGFRvIII* treated by fluoxetine (n= 4).
(B and C) Colony formation of U87EGFRvIII cells in soft agar (n= 4).
(D) Representative images of NHA and GBM spheres after DMSO or fluoxetine treatment. Scale bar, 500 μm.
(E) Representative flow cytometry analysis of Propidium iodide (PI) and Annexin V positive cells after DMSO or fluoxetine treatment.
(F) Relative mRNA level of *SMPD1* with its overexpression in (E).
(G) shRNA knockdown efficiency of *SMPD1*, *SCL6A4*, and *HTR2C* in U87EGFRvIII cells.
(H) mRNA level (RSEM) in GBM patient samples (TCGA).
(I) Rank of genes with the association (hazard ratio) between mRNA expression and overall survival of GBM patients from the TCGA dataset.
(J and K) Lipidomic analysis of U87 cells with or without EGFRvIII expression (n= 3).

(L-N) Relative cell viability in NHA and GBM cells (L) and colony formation in soft agar in U87EGFRvIII cells (M and N) treated with myriocin, an inhibitor of sphingolipid *de novo* synthesis.
(O and P) Crystal violet staining for U87 cells expressing EGFRvIII (n= 4).
(Q) Percentage of cell death of U87 cells with or without *EGFRvIII* overexpression after *SMPD1* or non-targeting shRNA transfection (n= 3).
(R) Relative mRNA level of *SMPD1* in three patient-derived GBM lines with indicated shRNA transfection.
For (F), a two-tailed Student's t-test was performed. ANOVA followed by Tukey's multiple comparisons test was applied in (C), (G), (H), (N), and (P-R). Data represent mean± SD except (H). The median value (center line) and the 25th and 75th percentiles (dash lines) are presented in (H).
**p < 0.01; ***p < 0.001.

Figure S3

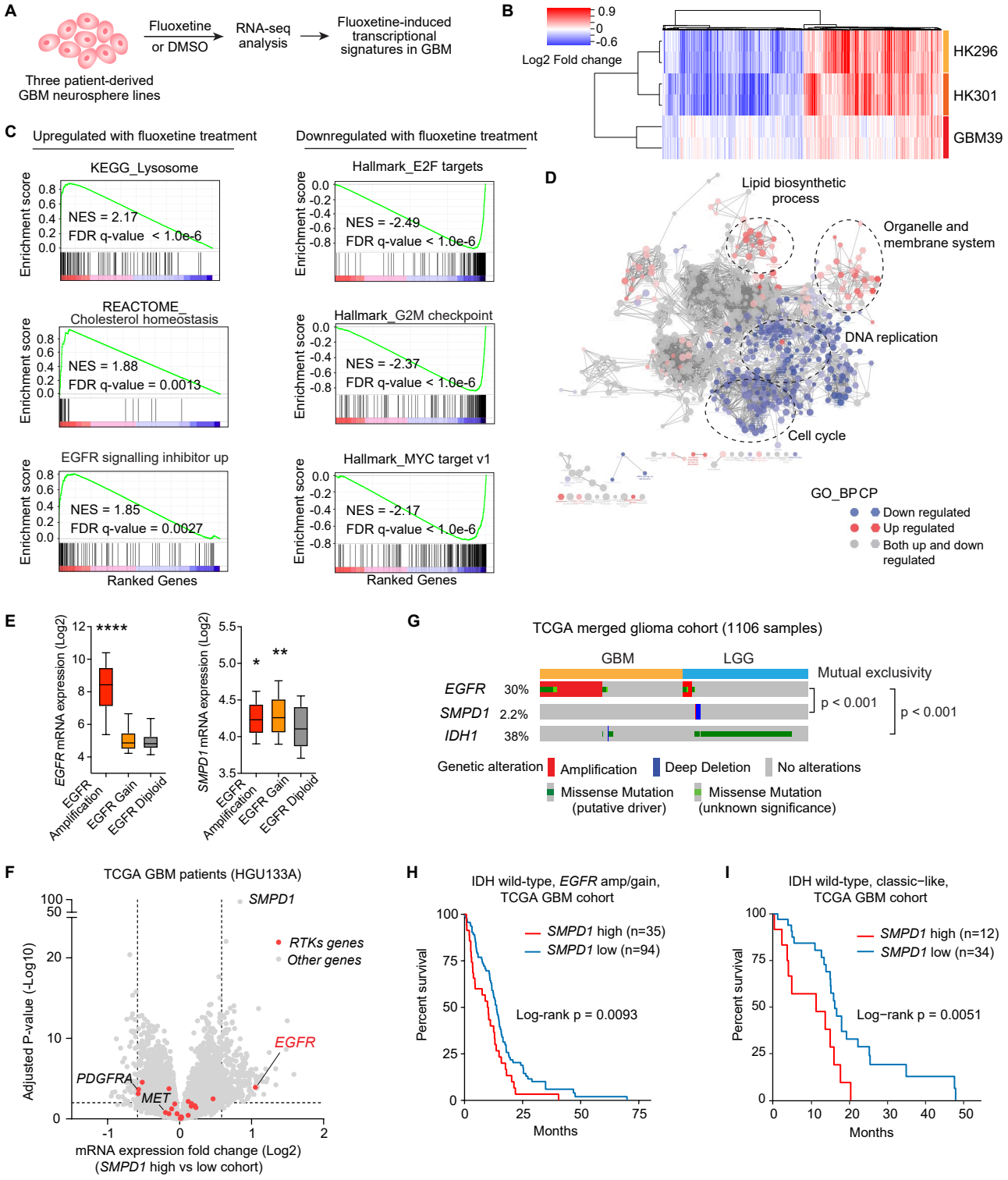

Figure S3. Fluoxetine-Induced Transcriptional Signatures in GBM Cells, Related to Figure 2

(A) Schematic overview of RNA-seq analysis in 3 GBM neurosphere lines with 42 hours DMSO or fluoxetine treatment. Two biological replicates per treatment were performed for each cell line.

(B) Heatmap of differentially expressed genes (FDR < 0.05) between fluoxetine and DMSO treatment in GBM39, HK296, and HK301 cells.

(C) Selected most significantly upregulated or downregulated transcriptional signatures by GSEA. FDR q-value and NES are shown.

(D) Gene Ontology (GO) enrichment analysis showing both upregulated and downregulated transcriptional signature clusters.

(E) *EGFR* and *SMPD1* mRNA level in GBM clinical samples of TCGA GBM (HUG133A) cohort.

(F) Volcano plot of differentially expressed genes in TCGA GBM clinical samples (HUG133A) with high or low *SMPD1* expression. RTKs genes are labeled as red.

(G) Genetic alterations of *EGFR*, *SMPD1*, and *IDH1* in merged LGG and GBM cohort of TCGA pan-cancer dataset (1106 samples). Deep deletion of *SMPD1* is mutually exclusively associated with *EGFR* amplification and gain of function mutations in clinical tumor samples.

(H) Kaplan-Meier analysis of overall survival in the wild-type IDH1 GBM patients with high or low *SMPD1* mRNA expression in EGFR amplification/ gain cohort of TCGA RNAseq dataset. The cutoff for high and low *SMPD1* expression cohorts is 10.60.
(I) Kaplan-Meier analysis of overall survival in wild-type IDH1 GBM patients with high (top 25%) or low *SMPD1* (bottom 75%) mRNA expression in the classic-like cohort of TCGA RNAseq dataset.
For (E), the median value (center line), the min and max (whiskers), and the 25th and 75th percentiles (box perimeters) are presented. ANOVA followed by Tukey's multiple comparisons test for (E), two-tailed Student's t-test for (F), Fisher's exact test for (G), and Log-rank test for (H) and (I). *p < 0.05; **p < 0.01; ****p < 0.0001.

Figure S4

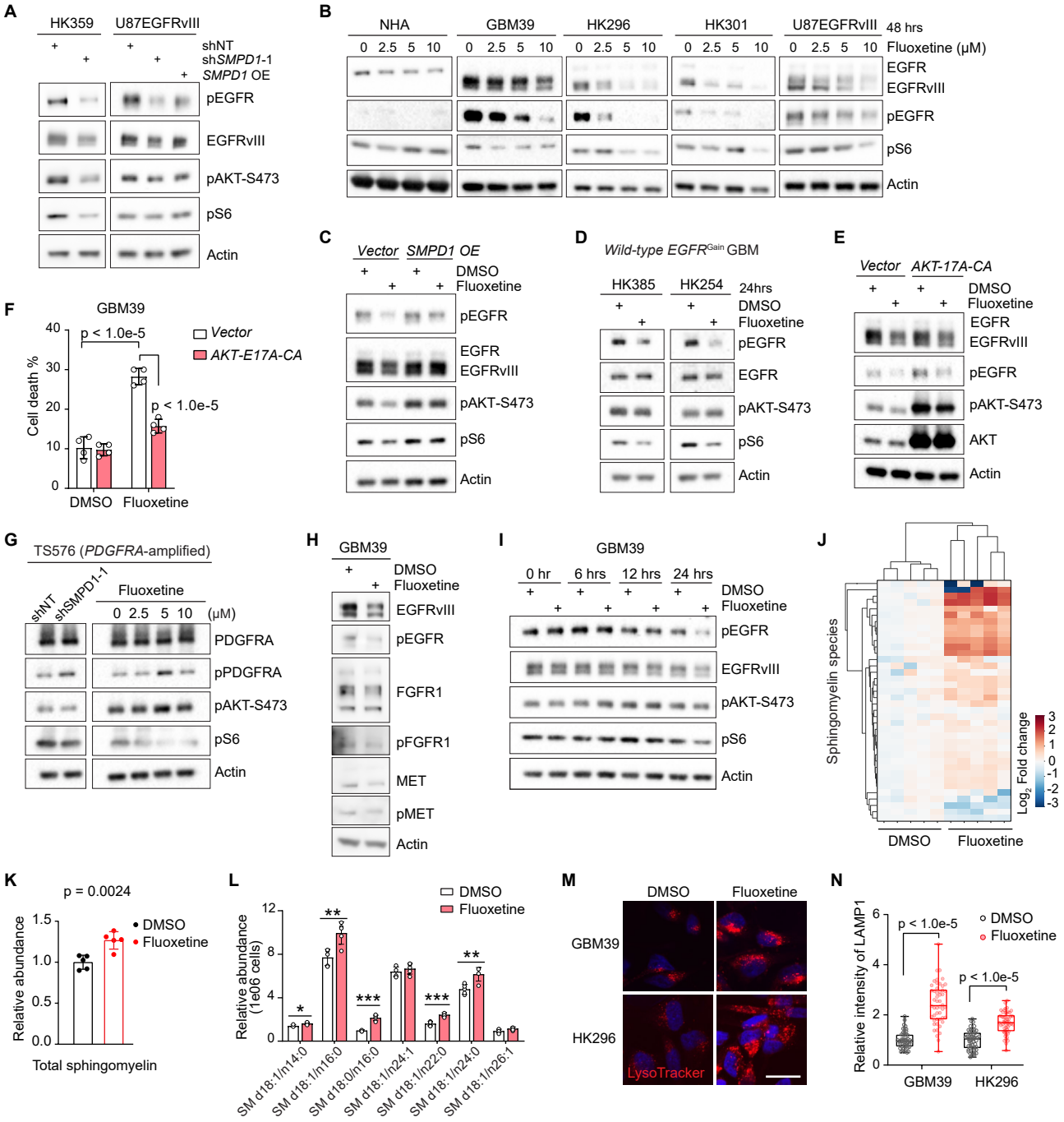

Figure S4. Fluoxetine Acts as an Indirect Inhibitor of EGFRvIII by Blocking SMPD1 and Elevating Sphingomyelin Levels, Related to Figure 2

(A) Western blot analysis of EGFR signaling activity in GBM cells expressing non-targeting (NT) or *SMPD1* shRNA.
(B) Western blot analysis of EGFR signaling activity in normal human astrocytes (NHA) and GBM cells after 48 hours of fluoxetine treatment.
(C) Western blot showing EGFR and downstream signaling in U87EGFRvIII cells with indicated treatment and gene expression.
(D) Western blot analysis of EGFR signaling activity in HK385 and HK254 cells after 24 hours of fluoxetine treatment.
(E and F) AKT signaling and percentage of cell death in GBM39 cells expressed vector or a constitutively active AKT E17A-CA allele (n= 4).
(G) Western blot showing PDGFRA and downstream signaling in TS576 cells with indicated treatment or shRNA expression.
(H) Western blot analysis of EGFR, FGFR1, and MET activity in GBM39 cells with 24 hours of indicated treatment.
(I) Western blot analysis of EGFR signaling activity in GBM39 cells treated with DMSO or 5 μM fluoxetine for indicated hours.
(J-L) Sphingomyelin profiles identified by mass spectrometry in U87EGFRvIII cells with 42 hours of DMSO or fluoxetine treatment (n=5).
(M) LysoTracker staining in GBM39 and HK296 cells. LysoTracker, red; DAPI, blue. Scale bar, 20 μm.
(N) Quantification of LAMP1 intensity in GBM39 and HK296 cells (n= 50).
Data represent mean± SD in (F), (K), and (L). The median value (center line), the min and max (whiskers), and the 25th and 75th percentiles (box perimeters) are presented in (N). Two-tailed Student's t-test for (K), (L), and (N). ANOVA followed by Tukey's multiple comparisons test for (F). *p < 0.05; **p < 0.01; ***p < 0.001.

Figure S5

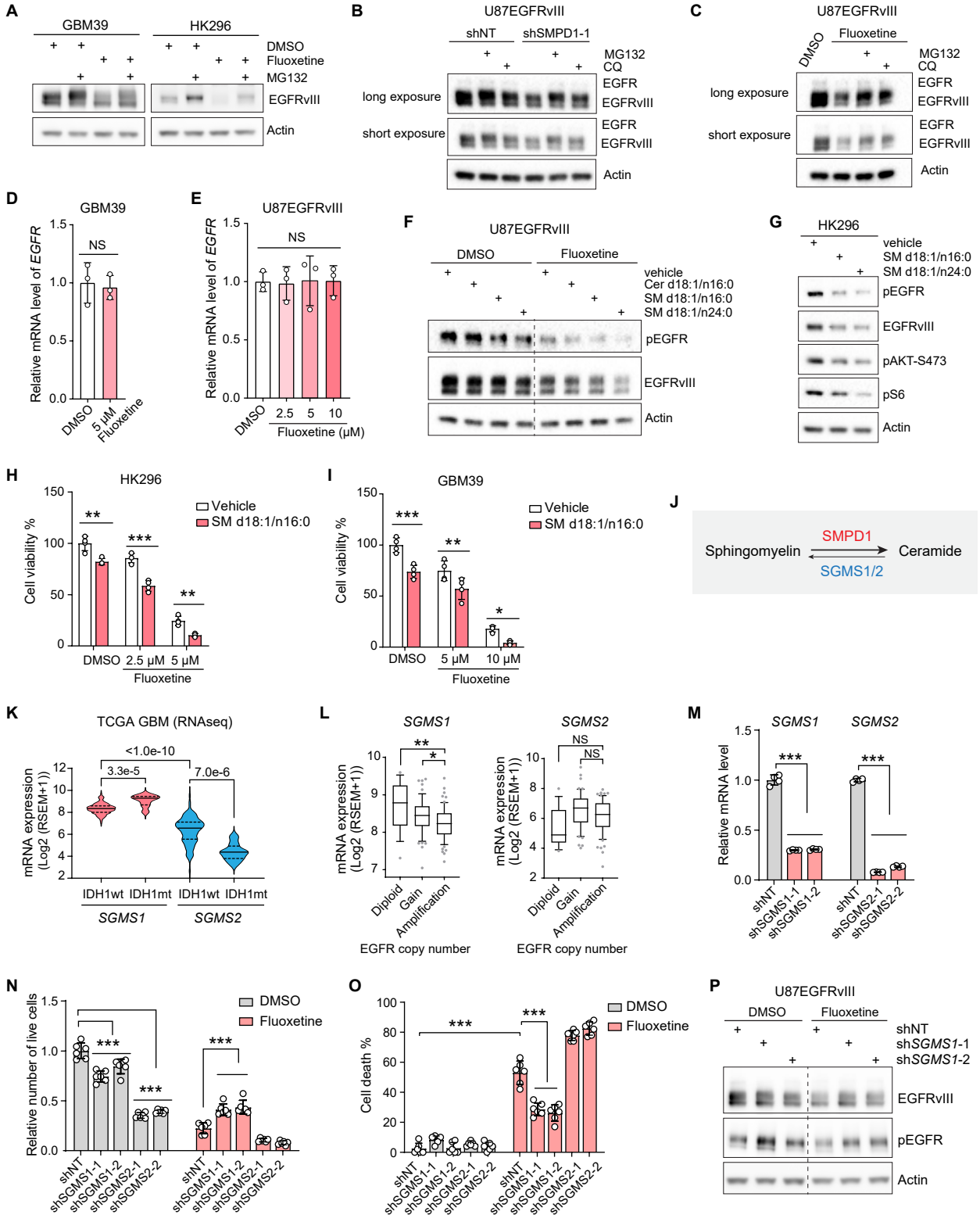

Figure S5. Fluoxetine Kills GBM Cells by Inhibiting SMPD1 and Abrogating EGFRvIII Signaling, Related to Figure 3

(A) Western blot analysis of EGFR protein in GBM39 and HK296 cells with indicated treatment and further incubated for additional 6 hours in the absence or presence of MG132.

(B and C) Western blot analysis of EGFR protein in U87EGFRvIII cells with indicated treatment and further incubated for additional 6 hours in the absence or presence of MG132 or Chloroquine (CQ).

(D and E) Relative *EGFR* mRNA level in GBM cells with 48 hours of fluoxetine treatments (n= 3).

(F-I) Adding sphingomyelins, but not ceramides, suppresses EGFR signaling (F and G) and further decreases cell viability (H and I) in GBM cells (n= 4).

(J) Schematic pathway of roles of SMPD1 and SGMS1/2 in regulating sphingomyelin homeostasis.
(K and L) mRNA expression of *SGMS1* and *SGMS2* in indicated cohorts of TCGA GBM (RNAseq) dataset.
(M) Knockdown efficiency of *SGMS1* and *SGMS2* shRNAs in U87EGFRvIII cells (n= 4).
(N-P) Relative number of live cells (N), percentage of cell death (O), and EGFR activity (P) in U87EGFRvIII cells with indicated treatments and shRNA expression (n= 6).
Data represent mean± SD except (K) and (L). The median value (center line), the min and max (whiskers), and the 25th and 75th percentiles (box perimeters) are presented in (K) and (L). Two-tailed Student's t-test for (D) and (K). ANOVA followed by Tukey's multiple comparisons test for (E), (H), (I), and (L-O). *$p < 0.05$; **$p < 0.01$; ***$p < 0.0001$; NS, not significant.

Figure S6

A

FDA-approved fluoxetine doses for human non-cancer indications (mg/day)	Mice doses converted from human doses based on body surface area (mg/kg/day)
20	4.2
40	8.2
50	10.2
60	12.3
80	16.4

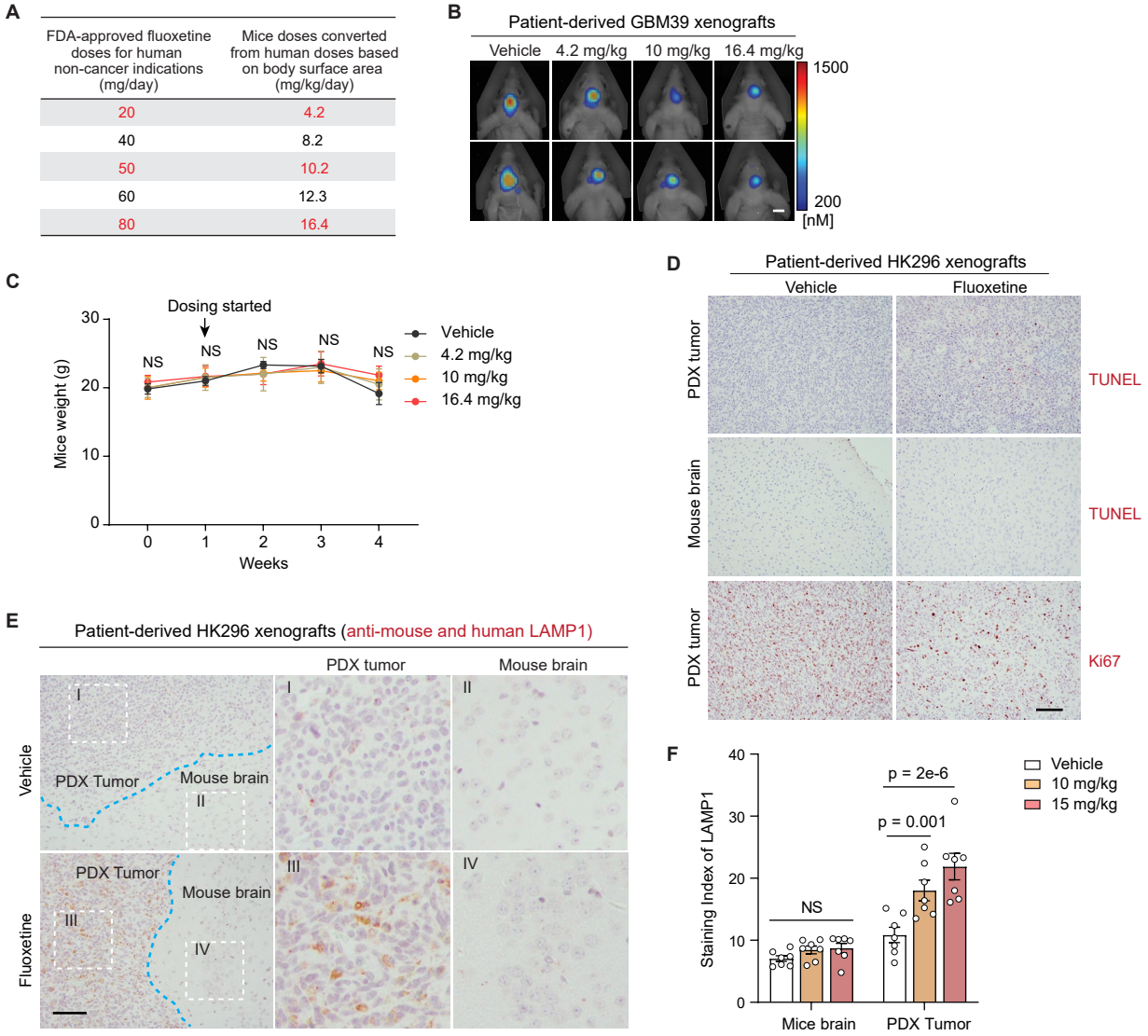

Figure S6. Fluoxetine Suppresses Tumor Growth in Patient-Derived Orthotopic GBM Models, Related to Figure 4

(A) FDA-approved doses of fluoxetine for human non-cancer indications and converted mice doses based on body surface area.

(B) Representative tumor images of GBM39 patient-derived orthotopic mice models. Scale bar, 5 mm.

(C) Body weights of mice bearing patient-derived GBM39 xenograft models with indicated administrations (n= 6 per group). Data represent mean± SD.

(D) Representative images of immunohistochemistry analysis of TUNEL and Ki67 in HK296 xenograft tumors and surrounding mice brains. Scale bar, 100 μm.

(E and F) Immunohistochemistry analysis of LAMP1 in HK296 xenograft tumors and surrounding mice brains by using an antibody that could detect both human and mice LAMP1 proteins (n= 7). Scale bar, 100 μm. Data represent mean± SEM.

ANOVA followed by Tukey's multiple comparisons test in (C) and (F). NS, not significant.

Figure S7

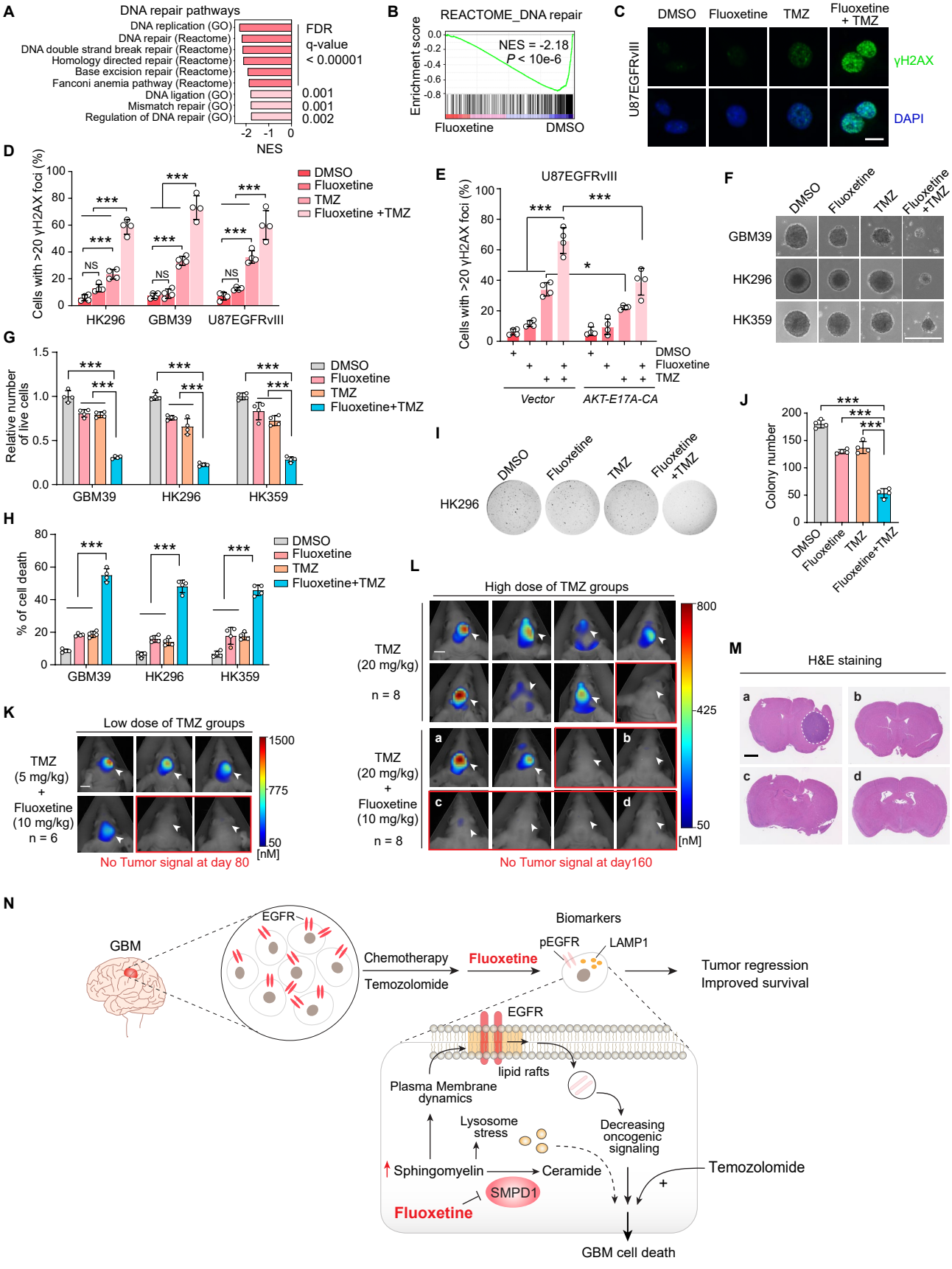
A
DNA repair pathways
DNA replication (GO)
DNA repair (Reactome)
DNA double strand break repair (Reactome)
Homology directed repair (Reactome)
Base excision repair (Reactome)
Fanconi anemia pathway (Reactome)
DNA ligation (GO)
Mismatch repair (GO)
Regulation of DNA repair (GO)
FDR q-value
< 0.00001
0.001
0.001
0.002
NES
B
REACTOME_DNA repair
Enrichment score
NES = -2.18
P < 10e-6
Fluoxetine
DMSO
C
DMSO
Fluoxetine
TMZ
Fluoxetine + TMZ
U87EGFRvIII
γH2AX
DAPI
D
Cells with >20 γH2AX foci (%)
DMSO
Fluoxetine
TMZ
Fluoxetine +TMZ
HK296
GBM39
U87EGFRvIII
E
U87EGFRvIII
Cells with >20 γH2AX foci (%)
DMSO
Fluoxetine
TMZ
Vector
AKT-E17A-CA
F
DMSO
Fluoxetine
TMZ
Fluoxetine +TMZ
GBM39
HK296
HK359
G
Relative number of live cells
DMSO
Fluoxetine
TMZ
Fluoxetine+TMZ
GBM39
HK296
HK359
I
DMSO
Fluoxetine
TMZ
Fluoxetine +TMZ
HK296
J
Colony number
DMSO
Fluoxetine
TMZ
Fluoxetine+TMZ
H
% of cell death
DMSO
Fluoxetine
TMZ
Fluoxetine+TMZ
GBM39
HK296
HK359
K
Low dose of TMZ groups
TMZ (5 mg/kg) + Fluoxetine (10 mg/kg) n = 6
[nM]
No Tumor signal at day 80
L
High dose of TMZ groups
TMZ (20 mg/kg) n = 8
TMZ (20 mg/kg) + Fluoxetine (10 mg/kg) n = 8
[nM]
No Tumor signal at day160
M
H&E staining
N
GBM
EGFR
Chemotherapy
Temozolomide
Fluoxetine
Biomarkers
pEGFR
LAMP1
Tumor regression
Improved survival
EGFR
lipid rafts
Plasma Membrane dynamics
Lysosome stress
Decreasing oncogenic signaling
Sphingomyelin
Ceramide
SMPD1
Fluoxetine
Temozolomide
GBM cell death

Figure S7. Combination of Fluoxetine and Temozolomide Induces DNA Damage and Suppresses GBM Tumor Recurrence, Related to Figure 5 and 6

(A and B) Downregulated DNA repair pathways in three patient-derived GBM neurosphere lines after fluoxetine treatment.

(C-E) γH2AX staining analysis of GBM cells. Data are from four replicate samples for each treatment. 2.5 μM for fluoxetine, and 50 μM for TMZ. Scale bar, 10 μm.

(F-H) Representative images (F), relative number of live cells (G), and percentage of cell death (H) of three GBM neurosphere lines after indicated treatment (n= 4). Scale bar, 500 μm.

(I and J) Colony formation of HK296 cells with indicated treatment in soft agar (n= 4). 2.5 μM for fluoxetine, and 50 μM for TMZ.

(K and L) Tumor images of mice with the combination treatment of fluoxetine and TMZ at day 80 or day 160 in GBM39 xenograft models. No tumor signal was identified in 2 mice of low dose TMZ (5 mg/kg) combination group and 6 mice of high dose TMZ (20 mg/kg) combination group. Arrowheads indicate the injection sites of tumor cells. Scale bar, 5 mm.

(M) H&E staining of brain sections in (L) from mice bearing GBM39 xenograft tumors after indicated drug administration. Tumor regions are labeled by dashed lines. Scale bar, 1 mm.

(N) Schematic model of the fluoxetine's anti-GBM effect through SMPD1 inhibition. GBMs are highly dependent on SMPD1 for survival, which is enhanced in *EGFRvIII*-amplified tumors. Fluoxetine kills GBM cells by indirectly inhibiting EGFRvIII by elevating sphingomyelin levels to alter plasma membrane organization, and by causing lysosomal stress. Fluoxetine can be combined with temozolomide to suppress tumor recurrence, as detected in preclinical *in vivo* models and in electronic medical record data from patients.

Data represent mean± SD. ANOVA followed by Tukey's multiple comparisons test in (D), (E), (G), (H), and (J). *$p < 0.05$; ***$p < 0.001$; NS, not significant.

Table S2. List of ICD-9 and ICD-10 Codes Used to Define Initial Brain Cancer Cohort, Related to Figure 6.

ICD Code	ICD Version	Description
191	ICD-9	Malignant neoplasm of brain
1910	ICD-9	Malignant neoplasm of cerebrum, except lobes and ventricles
1911	ICD-9	Malignant neoplasm of frontal lobe
1912	ICD-9	Malignant neoplasm of temporal lobe
1913	ICD-9	Malignant neoplasm of parietal lobe
1914	ICD-9	Malignant neoplasm of occipital lobe
1915	ICD-9	Malignant neoplasm of ventricles
1916	ICD-9	Malignant neoplasm of cerebellum nos
1917	ICD-9	Malignant neoplasm of brain stem
1918	ICD-9	Malignant neoplasm of other parts of brain
1919	ICD-9	Malignant neoplasm of brain, unspecified
C71	ICD-10	Malignant neoplasm of brain
C710	ICD-10	Malignant neoplasm of cerebrum, except lobes and ventricles
C711	ICD-10	Malignant neoplasm of frontal lobe
C712	ICD-10	Malignant neoplasm of temporal lobe
C713	ICD-10	Malignant neoplasm of parietal lobe
C714	ICD-10	Malignant neoplasm of occipital lobe
C715	ICD-10	Malignant neoplasm of cerebral ventricle
C716	ICD-10	Malignant neoplasm of cerebellum
C717	ICD-10	Malignant neoplasm of brain stem
C718	ICD-10	Malignant neoplasm of overlapping sites of brain
C719	ICD-10	Malignant neoplasm of brain, unspecified

Table S3. Baseline Characteristics of The GBM Enriched Cohort, Related to Figure 6.

	No SSRI (N=182)	Any SSRI (N=56)	Fluoxetine (N=10)	Citalopram (N=13)	Escitalopram (N=38)	All Patients (N=238)
Age						
Mean (SD)	54.3 (10.2)	52.4 (11.8)	54.9 (8.60)	45.8 (11.8)	53.4 (12.5)	53.9 (10.6)
Median [Min, Max]	56 [23, 80]	56 [24, 80]	57 [42, 71]	45 [28, 63]	57 [24, 80]	56 [23, 80]
Age group						
18-40	16 (8.8%)	10 (17.9%)	0 (0%)	5 (38.5%)	7 (18.4%)	26 (10.9%)
41-60	114 (62.6%)	31 (55.4%)	8 (80%)	7 (53.8%)	18 (47.4%)	145 (60.9%)
above 60	52 (28.6%)	15 (26.8%)	2 (20%)	1 (7.7%)	13 (34.2%)	67 (28.2%)
Sex						
Female	70 (38.5%)	30 (53.6%)	9 (90%)	6 (46.2%)	19 (50%)	100 (42%)
Male	112 (61.5%)	26 (46.4%)	1 (10%)	7 (53.8%)	19 (50%)	138 (58%)
Baseline (pre-GBM) follow-up days						
Mean (SD)	1090 (844)	1000 (791)	930 (883)	1280 (912)	843 (695)	1070 (831)
Median [Min, Max]	883 [90, 3720]	889 [96, 3480]	726 [96, 2770]	1120 [227, 3300]	802 [96, 3480]	883 [90, 3720]
Charlson comorbidity score*						
Mean (SD)	0.511 (0.785)	0.357 (0.554)	0.400 (0.516)	0.308 (0.480)	0.368 (0.589)	0.475 (0.739)
Median [Min, Max]	0 [0, 4.0]	0 [0, 2.0]	0 [0, 1.0]	0 [0, 1.0]	0 [0, 2.0]	0 [0, 4.0]
Charlson comorbidity index*						
0	115 (63.2%)	38 (67.9%)	6 (60.0%)	9 (69.2%)	26 (68.4%)	153 (64.3%)
1-2	64 (35.2%)	18 (32.1%)	4 (40.0%)	4 (30.8%)	12 (31.6%)	82 (34.5%)
3-4	3 (1.6%)	0 (0%)	0 (0%)	0 (0%)	0 (0%)	3 (1.3%)
>=5	0 (0%)	0 (0%)	0 (0%)	0 (0%)	0 (0%)	0 (0%)
Elixhauser comorbidity score*						
Mean (SD)	1.26 (1.51)	1.14 (1.21)	1.10 (1.37)	0.923 (1.32)	1.16 (1.13)	1.24 (1.44)
Median [Min, Max]	1.0 [0, 7.00]	1.0 [0, 4.00]	0.5 [0, 4.0]	0 [0, 4.0]	1.0 [0, 4.0]	1.0 [0, 7.0]
Elixhauser comorbidity index*						
<0	0 (0%)	0 (0%)	0 (0%)	0 (0%)	0 (0%)	0 (0%)
0	74 (40.7%)	22 (39.3%)	5 (50.0%)	7 (53.8%)	13 (34.2%)	96 (40.3%)
1-4	98 (53.8%)	34 (60.7%)	5 (50.0%)	6 (46.2%)	25 (65.8%)	132 (55.5%)
>=5	10 (5.5%)	0 (0%)	0 (0%)	0 (0%)	0 (0%)	10 (4.2%)

*For each patient, the Charlson and the Elixhauser comorbidity indices were computed using ICD codes from their diagnostic history up to six months prior to the index GBM diagnosis.

Table S4. Baseline Characteristics of The Propensity Score-matched GBM Enriched Cohort, Related to Figure 6.

	Fluoxetine		Citalopram		Escitalopram	
	Treated (N=10)	**Non treated (N=20)**	**Treated (N=13)**	**Non treated (N=26)**	**Treated (N=38)**	**Non treated (N=76)**
Age						
Mean (SD)	54.9 (8.6)	54.8 (10.9)	45.8 (11.8)	46.1 (12.1)	53.4 (12.5)	53.8 (10.4)
Median [Min, Max]	57 [42, 71]	58 [24, 68]	45 [28, 63]	46 [28, 64]	57.5 [24, 80]	56 [28, 78]
Sex						
Female	9 (90%)	18 (90%)	6 (46.2%)	10 (38.5%)	19 (50%)	38 (50%)
Male	1 (10%)	2 (10%)	7 (53.8%)	16 (61.5%)	19 (50%)	38 (50%)
Elixhauser comorbidity score*						
Mean (SD)	1.10 (1.07)	1.10 (1.37)	0.923 (1.32)	0.962 (1.18)	1.16 (1.13)	1.18 (1.23)
Median [Min, Max]	1 [0, 3]	0.5 [0, 4.0]	0 [0, 4.0]	1 [0, 4.0]	1 [0, 4.0]	1 [0, 4.0]
Elixhauser comorbidity index*						
<0	0 (0%)	0 (0%)	0 (0%)	0 (0%)	0 (0%)	0 (0%)
0	5 (50%)	7 (35%)	7 (53.8%)	12 (46.2%)	13 (34.2%)	31 (40.8%)
1-4	5 (50%)	13 (65%)	6 (46.2%)	14 (53.8%)	25 (65.8%)	45 (59.2%)
>=5	0 (0%)	0 (0%)	0 (0%)	0 (0%)	0 (0%)	0 (0%)

*For each patient, Charlson and Elixhauser comorbidity indices were computed using ICD codes from their diagnostic histories up to six months prior to the index GBM diagnosis. The propensity score matching was performed using R “Matchit’ package (version 3.0.2) based on age, sex, and Elixhauser comorbidity score by matching two non-exposed subjects (GBM patients not treated with SSRI) against each exposed subject (SSRI treated GBM patient).

Table S5. Cox Proportional Hazards Regression Results for All-cause In-patient Mortality after Adjusting for Age, Sex, Elixhauser Comorbidity Index Score, and Using Time-dependent SSRI Exposures, Related to Figure 6.

Characteristic	Fluoxetine			Citalopram			Escitalopram		
	HR[1]	95% CI[1]	p-value	HR[1]	95% CI[1]	p-value	HR[1]	95% CI[1]	p-value
Age	1.03	1.01, 1.05	**<0.001**	1.03	1.01, 1.05	**<0.001**	1.03	1.01, 1.04	**0.001**
Sex									
F	—	—		—	—		—	—	
M	0.93	0.69, 1.27	0.67	0.89	0.66, 1.19	0.42	0.91	0.68, 1.21	0.51
`Elixhauser score`	1.07	0.97, 1.17	0.17	1.11	1.01, 1.21	**0.034**	1.06	0.97, 1.16	0.20
Fluoxetine									
No	—	—							
Yes	0.42	0.20, 0.88	**0.022**						
Citalopram									
No				—	—				
Yes				1.03	0.49, 2.19	0.94			
Escitalopram									
No							—	—	
Yes							1.11	0.71, 1.74	0.65

[1] HR = Hazard Ratio, CI = Confidence Interval

Table S6. Results of Cox Proportional Hazards Regression from 1:2 Matched Cohort (Two Non-SSRI Treated Patients for Each SSRI Treated Patient) and Adjusting for Age, Sex, Elixhauser Comorbid Score, and Treating SSRI Exposures as Time-dependent Variables, Related to Figure 6.

	Fluoxetine			Citalopram			Escitalopram		
Characteristic	**HR[1]**	**95% CI[1]**	**p-value**	**HR[1]**	**95% CI[1]**	**p-value**	**HR[1]**	**95% CI[1]**	**p-value**
Age	1.03	1.00, 1.07	**0.046**	1.02	0.99, 1.05	0.20	1.03	1.01, 1.06	**0.006**
Sex									
F	—	—		—	—		—	—	
M	3.24	1.17, 8.94	**0.023**	1.12	0.59, 2.13	0.73	1.00	0.67, 1.49	>0.99
`Elixhauser score`	1.21	0.89, 1.66	0.22	1.18	0.78, 1.79	0.43	0.98	0.85, 1.13	0.82
Fluoxetine									
No	—	—							
Yes	0.33	0.13, 0.86	**0.023**						
Citalopram									
No				—	—				
Yes				1.46	0.74, 2.91	0.28			
Escitalopram									
No							—	—	
Yes							1.43	0.91, 2.24	0.12

[1] HR = Hazard Ratio, CI = Confidence Interval